The International Symposium on Micro-Mechanical Engineering
December 1-3, 2003

ISMME2003-109

EFFECT OF CARBON ISOTOPE ABUNDANCE ON THERMAL CONDUCTIVITY AND RAMAN SCATTERING OF SINGLE-WALLED CARBON NANOTUBES

Shigeo MARUYAMA, Yuhei MIYAUCHI and Yuki TANIGUCHI
Department of Mechanical Engineering, The University of Tokyo
7-3-1 Hongo, Bunkyo-ku, Tokyo 113-8656, Japan.
TEL: 03-5841-6421, E-Mail: maruyama@photon.t.u-tokyo.ac.jp

Since there is about 1 % of ^{13}C isotope in natural abundance of carbon atoms, normal carbon nanotubes are made of carbon atoms with different masses. The vibrational features of single-walled carbon nanotubes (SWNTs) due to the isotope effect were studied through the alcohol catalytic CVD (ACCVD) generation and resonant Raman scattering of isotopically modified SWNTs, and through molecular dynamics simulations of phonon density of states (DOS) and heat conduction. SWNTs with various amount of ^{13}C abundance were generated by ACCVD technique from isotopically modified ethanol: $^{13}CH_3$-$^{13}CH_2$-OH, $^{13}CH_3$-CH_2-OH, and CH_3-$^{13}CH_2$-OH. The Raman scattering of these SWNTs showed a simple shift of Raman scattering frequency for ^{13}C SWNTs. By comparing the change in Raman spectra for ^{13}C and ^{12}C mixture cases, it was concluded that about a half of C-O bond of an original ethanol is completely broken at the decomposition process of ethanol. Those Raman features were compared with phonon DOS calculated with molecular dynamics method. Furthermore, by molecular dynamics simulations, thermal conductivity of SWNTs with randomly distributed ^{13}C with various ratios was calculated. A preliminary result showed that the dependency of thermal conductivity on isotope ratio was well explained with a simple phonon scattering model.

Keywords: *Single-Walled Carbon Nanotubes, Isotope, Alcohol CCVD, Molecular Dynamics Method, Thermal Conductivity*

INTRODUCTION

The discovery of single-walled carbon nanotubes (SWNTs) in 1993 [1] was one of the most important event in the nanotechnology of this century. Many exciting physical properties of this new form of carbon have been revealed [2, 3]. Among them, vibrational features and issues of heat conduction are considered in this paper. It is well-known that the inclusion of only 1 % of ^{13}C natural isotope dramatically reduces the thermal conductivity of isotopically pure diamond [4]. The normal carbon atoms are composed of isotope mixtures of natural abundance, i.e. 98.892% ^{12}C and 1.108% ^{13}C. Hence, normal carbon nanotubes are made of carbon atoms with different masses. Since the extremely high thermal conductivity is predicted [5] for carbon nanotubes, the deterioration of thermal conductivity by the isotope effect is quite a concern. However, the previous molecular dynamics result suggested that the isotope effect was negligible for carbon nanotubes [5]. The isotope effect on thermal conductivity and phonon vibrational mode is not yet clearly assigned from molecular dynamics level. In this report, the vibrational features of single-walled carbon nanotubes (SWNTs) due to the isotope effect are studied through the alcohol catalytic CVD (ACCVD) generation and resonant Raman scattering of isotopically modified SWNTs, and through molecular dynamics simulations of phonon density of states (DOS) and heat conduction.

By ACCVD technique developed in our group [6-11], high-purity SWNTs can be generated at low temperature with a simple experimental apparatus. In this report, ACCVD method is modified for the efficient production of SWNTs from very small amount of ethanol with the similar technique used for the SWNTs generation from fullerene [12]. The SWNTs with various amount of ^{13}C abundance were generated by ACCVD technique from isotopically modified ethanol: $^{13}CH_3$-$^{13}CH_2$-OH, $^{13}CH_3$-CH_2-OH, and CH_3-$^{13}CH_2$-OH, in addition to the normal ethanol. The resonant Raman scattering of those SWNTs shows a simple shift of Raman scatting frequency for ^{13}C SWNTs and a meaningful shift and broadening for ^{12}C and ^{13}C mixture cases. Those features are compared with phonon density of states calculated with molecular dynamics method [13-15].

We have been studying the heat conduction characteristics along an SWNT by the molecular

dynamics method [13-15] with the simplified form [16] of Tersoff-Brenner bond order potential [17]. Our preliminary results showed that thermal conductivity was strongly dependent on the nanotube length for realistic length scale for device applications. Furthermore, we have reported the direct calculation of phonon dispersion relations and phonon density of states from molecular dynamics trajectories [13-15]. The calculated thermal conductivity for a finite length nanotube was not as high as the previously reported result that it might be as high as 6600 W/mK at 300 K [5]. However, the thermal conductivity was much higher than high-thermal conductivity metals.

In order to clarify the isotope effect on heat conduction and on Raman scattering, thermal conductivity and phonon DOS of nanotube with randomly distributed ^{13}C with various ratios was calculated. A preliminary result showed that the dependency of thermal conductivity on isotope ratio was well explained with a simple phonon scattering model.

NOMENCLATURE

a : Translation lattice vector
$a_{c\text{-}c}$: Bond length of carbon, nm
b : van der Waals distance, 0.34 nm
c : Velocity of light, m/s
d : Diameter of nanotube, nm
$D(\omega)$: Phonon density of states
$\hbar$: Planck constant, Js
k : Wave vector, 1/nm
k_B : Boltzmann constant, J/K
L : Length of a SWNT, nm
m_{ave} : Average mass, amu
P_{free} : Probability of C-O bond break
q : Heat flux, W/m^2
r : Cylindrical coordinate (radial direction), nm
T : Temperature, K
t : Time, s
v : Velocity, m/s
x, y, z : Cartesian coordinates (z is along tube axis), nm

Greek Symbols
α : Ratio of site 1 carbon atom, or running index
β : Ratio of ^{13}C atoms
λ : Thermal conductivity, W/mK
θ : Azimuth angle

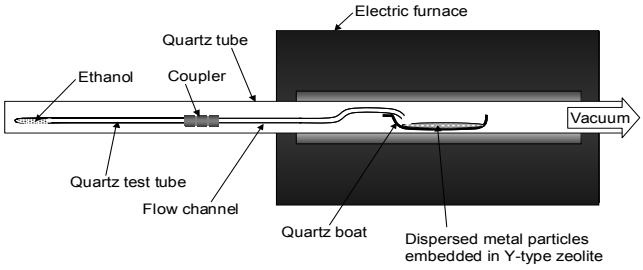

Fig. 1 Schematic diagram of experimental apparatus.

ν : Frequency, Hz
ν' : Wave length $\nu'=\nu/c$, cm^{-1}
ω : Radial frequency $\omega = 2\pi\nu$, 1/s

GENERATION OF ISOTOPICALLY MODIFED SWNTS

Alcohol CCVD Method

The production technique of SWNTs has been developed from the landmark establishment of the synthesis method in macroscopic amount by laser-furnace [18] and arc-discharge methods [19]. Recently, several techniques employing CVD approach [20-24] has been proposed for the improved efficiency or productivity in the bulk synthesis of SWNTs. At present, CVD approaches including the high-pressure CO (HiPco) technique [21,22] have become dominant for the mass production of SWNTs. Recently, we have proposed the use of alcohol, especially ethanol and methanol, for the carbon feedstock [6,7]. The proposed ACCVD method can produce SWNTs with fine quality when combined with appropriate catalysts and experimental procedures. Furthermore, it was recently demonstrated that high quality SWNTs could be synthesized on the mesoporous-silica coated substrate [8] or directly on solid substrate such as silicon and quartz [9]. This versatile nature of this technique made it possible to use rather expensive isotopically modified ethanol for the production of SWNTs.

Experimental Procedure

The detailed preparation of metal supporting zeolite powder was described in our previous reports [6-11]. We prepared a catalytic powder by impregnating iron acetate

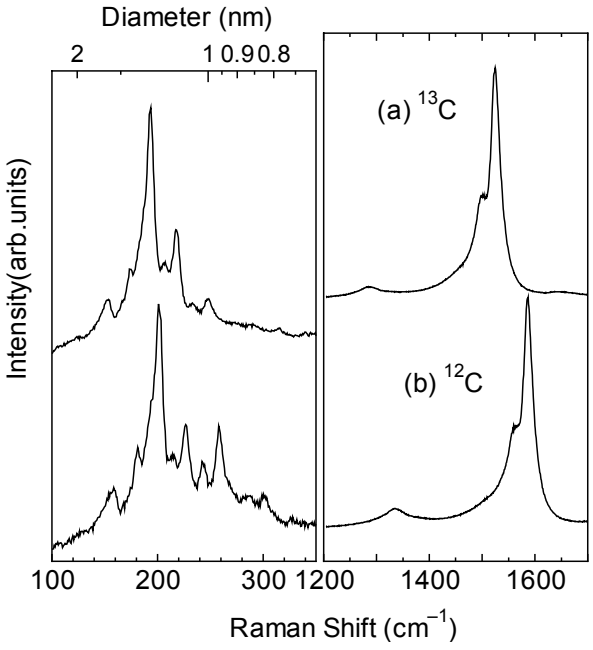

Fig. 2 Raman Scattering of SWNTs made of isotopically modified ethanol. (a) SWNTs generated from $^{13}CH_3$-$^{13}CH_2$-OH. (b) SWNTs from normal ethanol.

$(CH_3CO_2)_2Fe$ and cobalt acetate $(CH_3CO_2)_2Co\text{-}4H_2O$ onto USY-zeolite powder (HSZ-390HUA over 99 % SiO_2) [25, 26]. The weight concentration of Fe and Co was chosen to be 2.5 wt% each over the catalytic powder.

The schematic of our CVD apparatus and standard procedure of the CVD were presented in Refs. [10] and [9], respectively. Here, a slightly different apparatus and procedure is employed for the efficient production of SWNTs from small amount of ethanol [12]. The schematic of experimental apparatus is shown in Fig. 1. In brief, the catalyst was placed on a quartz boat and the boat was set in the center of a quartz tube (i.d. = 26 mm, length = 1 m). Small amount of ethanol was placed in an end of a smaller test-tube guiding the carbon source flow to the catalyst. One end of the quartz tube was connected to a rotary pump by two different paths, one 25 mm and the other 6 mm diameter tubes to select the pumping efficiency. The central 30 cm of the quartz tube was surrounded with an electric furnace. While the furnace was heated up from room temperature, about 200 sccm of Ar was flowed so that the inside of the quartz tube was maintained at 1 atm. After the electric furnace reached desired temperature, 800 °C, Ar flow was stopped and the larger evacuation path was opened to bring the inside of the quartz tube vacuum. Subsequently, ethanol vapor was injected to catalyst for 5 min. from the end of the smaller test-tube ethanol reservoir.

The synthesized SWNTs were characterized by micro Raman scattering measurements using CHROMEX 501is and ANDOR DV401-FI for the spectrometer and CCD system, respectively, with an optical system of SEKI TECHNOTRON STR250.

Isotopically Modified SWNTs

In addition to normal ethanol, 3 isotopically modified ethanol were employed for the production of isotopically modified SWNTs. Three isotopically modified ethanol were $^{13}CH_3\text{-}^{13}CH_2\text{-}OH$ (1,2-$^{13}C_2$, 99%), $^{13}CH_3\text{-}CH_2\text{-}OH$ (2-^{13}C, 99%), $CH_3\text{-}^{13}CH_2\text{-}OH$ (1-^{13}C, 98%), supplied from Cambridge Isotope Laboratories, Inc. The carbon atoms in normal ethanol $CH_3\text{-}CH_2\text{-}OH$ are composed of isotope mixtures of natural abundance, ie. 98.892% ^{12}C and 1.108% ^{13}C. Hence, by using normal ethanol, generated SWNTs should be composed of carbon atoms with the same abundance ratio. On the other hand, by using ethanol ($^{13}CH_3\text{-}^{13}CH_2\text{-}OH$), SWNTs principally made of ^{13}C can be generated. By using other 2 isotopically labeled ethanol ($^{13}CH_3\text{-}CH_2\text{-}OH$ or $CH_3\text{-}^{13}CH_2\text{-}OH$), the abundance of ^{13}C isotopes in generated SWNTs should depend on the reaction process. For isotopically modified ethanol, 0.5 g sample was used for the ACCVD source for production of sufficient amount of SWNTs for resonant Raman scatting

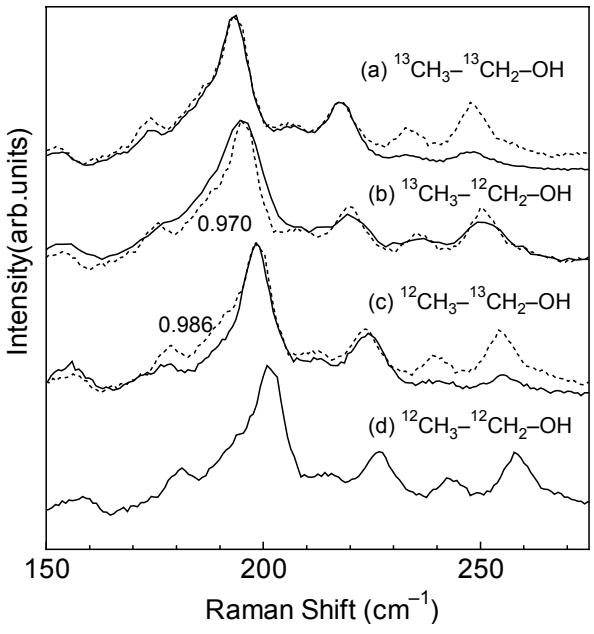

Fig. 3 Comparison of RBM mode of SWNTs generated from various isotopically modified ethanol. (a): SWNTs from $^{13}CH_3\text{-}^{13}CH_2\text{-}OH$. (b): SWNTs from $^{13}CH_3\text{-}^{12}CH_2\text{-}OH$. (c): SWNTs from $^{12}CH_3\text{-}^{13}CH_2\text{-}OH$. (d): normal ethanol, $^{12}CH_3\text{-}^{12}CH_2\text{-}OH$ (natural abundance of ^{13}C is included). Dotted lines: Shifted spectra of ^{12}C SWNTs. Following fitting factor was multiplied to the frequency: (a) $\sqrt{12/13}$, (b) 0.970, (c) 0.986.

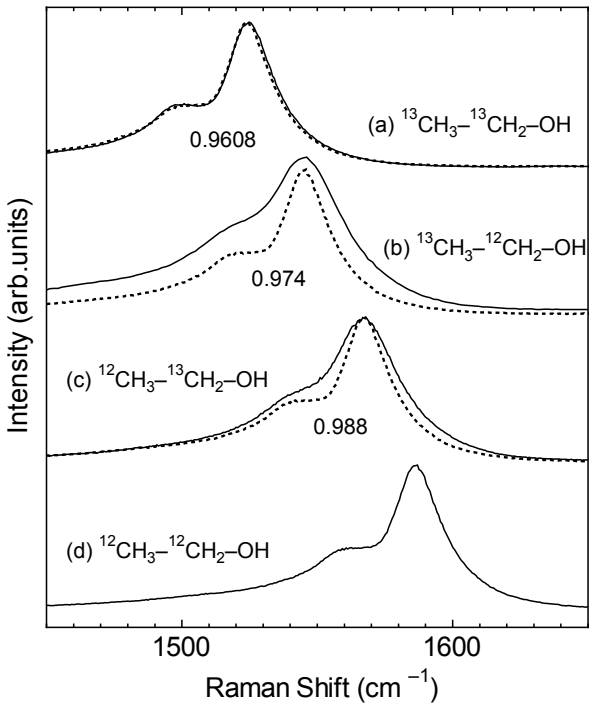

Fig. 4 Comparison of G-band of SWNTs generated from various isotopically modified ethanol. (a): SWNTs from $^{13}CH_3\text{-}^{13}CH_2\text{-}OH$. (b): SWNTs from $^{13}CH_3\text{-}^{12}CH_2\text{-}OH$. (c): SWNTs from $^{12}CH_3\text{-}^{13}CH_2\text{-}OH$. (d): normal ethanol, $^{12}CH_3\text{-}^{12}CH_2\text{-}OH$ (natural abundance of ^{13}C is included). Dotted lines: Shifted spectra of ^{12}C SWNTs. Following fitting factor was multiplied to the frequency: (a) $\sqrt{12/13}$, (b) 0.974, (c) 0.988.

experiments.

Change in Raman Spectra

Raman Scattering of ^{13}C SWNTs

Fig. 2 compares Raman scattering spectra for ^{13}C SWNT and normal SWNTs excited with 488 nm laser. Spread in G-band peak at 1590 cm^{-1} for normal SWNTs and smaller D-band signal at 1350 cm^{-1} suggest that high quality SWNTs were generated by these experiments from tiny amount of ethanol [27, 28]. The strong radial breathing mode (RBM) peaks at around 150-300cm^{-1} corresponding to the nanotube diameter confirms this observation. The corresponding diameter d (nm) of SWNTs calculated with $d = 248/\nu'$ from RBM frequency ν' (cm^{-1}) is shown on top axis [29, 30] . This relation is valid for normal SWNTs. There was no change in Raman spectra shape for ^{13}C SWNT but the Raman shift frequency was $\sqrt{12/13}$ times smaller because of the heavier carbon atoms.

Reaction Mechanism

Detailed shift in Raman spectra are summarized in Fig. 3 for RBM and in Fig. 4 for tangential mode. By multiplying the mass-ratio factor $\sqrt{12/13}$ =0.9608 to frequency of ^{12}C spectrum, ^{13}C spectrum is almost completely reproduced as in Fig. 3(a) and Fig. 4(a), where dotted line is the shifted spectrum from ^{12}C.

The interpretation of 2 mixed isotope cases in Figs. 3 (b, c) and 4 (b, c) is quite important. The difference in the vibrational frequency between (b) from $^{13}CH_3$-$^{12}CH_2$-OH and (c) from $^{12}CH_3$-$^{13}CH_2$-OH means that two carbon atoms in an ethanol molecule are not equally used for the SWNT formation. Apparently, the carbon atom at site 2, further from OH, is more likely to be incorporated into an SWNT. The amount of shift is clearly compared in Fig. 4. The scaling factor on frequency of the dotted lines for (b) and (c) were 0.974 and 0.988, respectively. Assuming that this factor is the frequency change due to the average mass of carbon atoms, the factor should equal to $\sqrt{12/m_{ave}}$. Then, the average mass for (b) and (c) are 12.65 amu (Site 1: Site 2 = 35:65) and 12.30 amu (Site 1: Site 2 = 30:70), respectively. Both (b), (c) results and also results in Fig. 3 all coincide that only 1/3 or 1/4 of carbon atoms in an SWNT is from the site 1 carbon atom. This result gives an important key for the analysis of the reaction mechanism of nanotube formation. On the metal catalyst surface, ethanol is expected to decompose. After losing hydrogen atoms, we believe that the oxygen atom has an important role of cleaning the carbon atoms with dangling bonds. This should be the most important point of ACCVD method. Here, the isotopically labeled experiments show that the original C-O bond in an ethanol molecule should break at least 30 to 35 % probability. Hence, it is certain that oxygen atom is sometime really becomes free and find some carbon atom which was not its previous partner.

Let's assume that the ratio of original site 1 carbon atom in an SWNT is α, and that of site 2 is $(1-\alpha)$. If we further assume that the probability of complete break of C-O bond is P_{free}, and the free oxygen atom can randomly find its partner to become gas phase CO. Then,

$$(1-\alpha)P_{free} = \alpha, \quad or \quad P_{free} = \frac{\alpha}{1-\alpha}. \qquad (1)$$

Then, P_{free} should be 42 to 54 %. So, we can conclude that half of C-O bond of an original ethanol is completely broken in ACCVD process.

In addition to the shift of the frequency, slight broadening of spectra was observed for the mixed isotope cases such as in Fig. 4(b, c). Here, it should be noted that for the Raman spectra in Fig. 4(b), lower resolution of frequency was used but the measurement resolution was same of Fig. 4(a), 4(c), and 4(d). More detailed discussions of the broadening is discussed later with the reference to the molecular dynamics simulation.

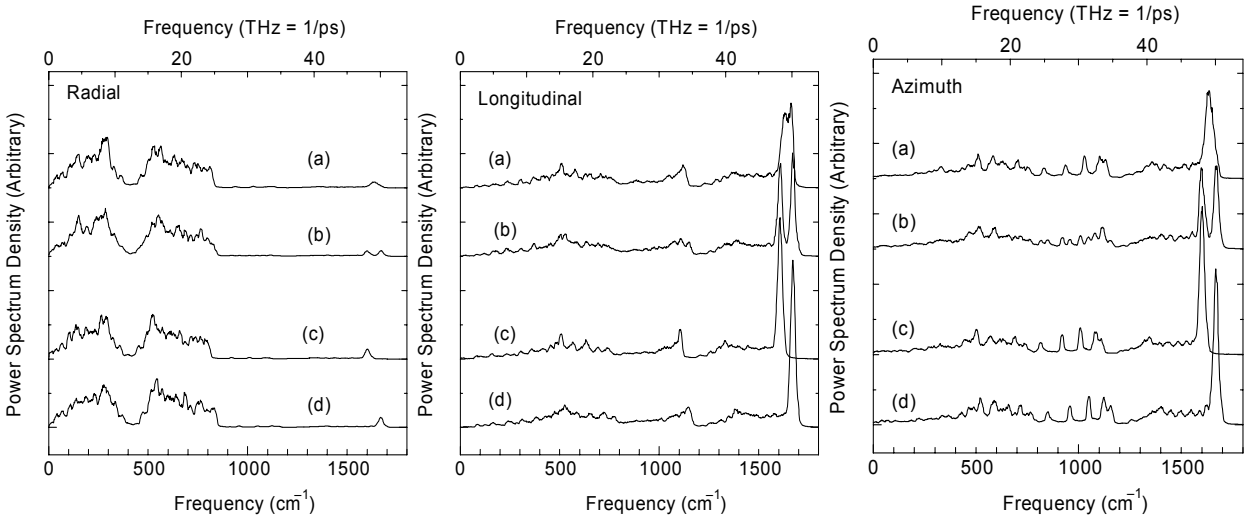

Fig. 5 Phonon density of states calculated by MD simulation. (a) 1:1 random mixture of ^{12}C and ^{13}C. (b) connection of ^{12}C nanotube and ^{13}C nanotube, (c) pure ^{13}C nanotube, (d) pure ^{12}C nanotube.

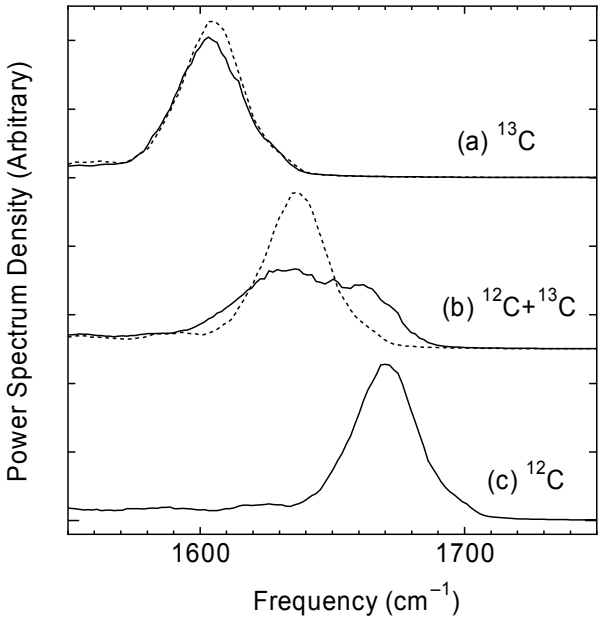

Fig. 6 Comparison of phonon DOS (average of longitudinal and azimuth directions for tangential mode range). (a) pure ^{13}C nanotube, (b) 1:1 mixture of ^{12}C and ^{13}C, (c) pure ^{12}C nanotube. Dotted lines: Shifted spectra of ^{12}C SWNTs. Following fitting factor was multiplied to the frequency: (a) $\sqrt{12/13}$, (b) 0.9798.

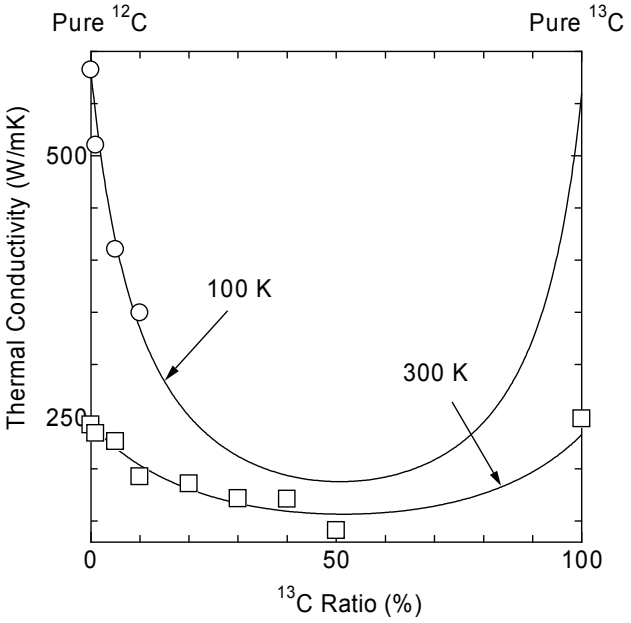

Fig. 7 Effect of ^{13}C isotope on thermal conductivity of SWNT

MOLECULAR DYNAMICS METHOD

Numerical Technique

For the comparison with the Raman spectra, phonon density of states (DOS) were calculated for nanotubes with randomly mixed ^{13}C isotopes. As the geometry of nanotubes, (10, 10) nanotube with length of 25 nm was employed. Except for the inclusion of ^{13}C isotopes of fixed amount at random positions, all simulation techniques are the same as our previous reports [14, 15]. Briefly, Brenner potential [17] with the simplified form [16] was employed as the potential function with the parameter set II (table 2 in [17]), which better reproduced the force constant. The velocity Verlet method was adopted to integrate the equation of motion with the time step of 0.5 fs. By applying the phantom heat bath model [31] to each end of a SWNT, the temperature difference was applied. While one unit-cell molecules were fixed, one unit-cell molecules next to them were controlled by the Langevin equation. Here, no periodic boundary condition was applied to handle the finite size effect of carbon nanotubes. For the normal infinite length simulation, it is often discussed that the cell length of periodic boundary condition should be larger than the "mean free path" of phonon, which is argued to be order of 1 μm.

Phonon Density of States (DOS)

Following our previous reports [14,15], phonon density of states was calculated as the power spectra of velocity fluctuations in Eq. (2).

$$D_\alpha(\omega) = \int dt \exp(-i\omega t)\langle v_\alpha(t) v_\alpha(0)\rangle \qquad (2)$$

Here, α takes r, θ, z for each velocity component in the cylindrical coordinate. The calculated density of states is shown in Fig. 5 for various mixing of ^{13}C isotopes. Even though the Raman active modes were not selected in Fig. 5, qualitative comparison with measured Raman spectra can be possible. Phonon DOS from radial components of velocity fluctuations includes the radial breathing mode (RBM) signal in Raman spectra, and that from longitudinal and azimuth directions include the tangential mode or G-band signal. G-band features are compared in Fig. 6 in the similar fashion as in Fig. 4. Comparing pure ^{12}C and pure ^{13}C spectra, the only difference must be the frequency shift by the factor of $\sqrt{12/13}$. The half and half mixture of ^{12}C and ^{13}C in Fig. 5 (a) shows the broader G-band signal compared with experimentally obtained broadening as in Fig. 4(c) with the average frequency almost consistent with the simple estimation of the shift ratio described as $\sqrt{12/12.5}$ =0.9798.

Thermal Conductivity

With our configuration, thermal conductivity was calculated from the measured temperature gradient and the heat flux obtained by the energy budgets of phantom molecules [14, 15]. After obtaining the average temperature of about 300 K or 100 K with the auxiliary velocity scaling control, typically 1 ns simulations were performed for the equilibration with only phantom temperature control. Then, 2 ns calculation was used for the measurement of temperature distribution, with 20 K temperature difference. With energy budgets of controlling phantom molecules, the heat flux along the tube can be simply calculated. Combined with the

temperature gradient, the thermal conductivity λ can be calculated through Fourier's equation: $q = -\lambda(\partial T / \partial z)$. As the definition of cross-sectional area, area of a hexagon dividing a bundle of SWNTs was used: $2\sqrt{3}\left(d/2 + b/2\right)^2$, where b is van der Waals thickness 0.34 nm. This definition is convenient for the comparison of thermal conductivity of an SWNT with a DWNT or a peapod. It should be noted that we used the area of a ring of van der Waals thickness: πbd in our previous reports [14, 15]. Hence, the absolute value of thermal conductivity is smaller in this report. Thermal conductivity of nanotube with randomly distributed ^{13}C with various ratios was calculated. A preliminary result is shown in Fig. 7. Here, (5, 5) nanotube with about 50 nm was used. The dependency of thermal conductivity on isotope ratio was well explained with the following equation as the fit curves in Fig. 7.

$$\lambda = \sqrt{\frac{12}{12(1-\beta)+13\beta}} \cdot \frac{\lambda_{pureC^{12}}}{C_1 \cdot \beta(1-\beta)+1} \qquad (3)$$

where β is the ratio of ^{13}C, $\lambda_{pureC^{12}}$ is the thermal conductivity for pure ^{12}C, C_1 is the fitting parameter. It is also noted that the thermal conductivity at 100 K is not realistic in Fig. 7 because the classical simulation cannot reproduce the correct change of heat capacity at low temperature [15]. The mechanism of the decrease of thermal conductivity with isotopes is discussed.

CONCLUSION

Alcohol catalytic CVD (ACCVD) generation of high-purity SWNTs was performed from isotopically modified ethanol: $^{13}CH_3$-$^{13}CH_2$-OH, $^{13}CH_3$-CH_2-OH, and CH_3-$^{13}CH_2$-OH. The Raman scattering of those SWNTs shows a simple shift of Raman scatting frequency for ^{13}C SWNTs and a meaningful shift and broadening for ^{12}C and ^{13}C mixture cases. By comparing the change in Raman spectra, it was concluded that about a half of C-O bond of an original ethanol is completely broken at the decomposition process of ethanol. By molecular dynamics simulations, thermal conductivity of SWNTs with randomly distributed ^{13}C with various ratios was calculated. A preliminary result showed that the dependency of thermal conductivity on isotope ratio was well explained with a simple phonon scattering model.

ACKNOWLEDGMENT

We thank Dr. T. Ishikura at Tokyo Gas Co., Ltd. for the insightful discussion of isotope effects on carbon nanotubes.

REFERENCES

[1] Iijima, S. and Ichihashi, T., "Single-Shell Carbon Nanotubes of 1-nm Diameter," Nature, vol. 363 (1993), pp. 603-605.

[2] Dresselhaus, M.S., Dresselhaus, G., Eklund, P.C., "Science of Fullerenes and Carbon Nanotubes," Academic Press, New York, 1996.

[3] Saito, R., Dresselhaus, G., Dresselhaus, M.S., "Physical Properties of Carbon Nanotubes," Imperial College Press, London, 1998.

[4] Plekhanov, V.G., "Isotope Effects on the Lattice Dynamics of Crystals," Materials Sci. Eng. R, vol. 35 (2001), pp.139-237.

[5] Berber, S., Kwon, Y.-K., Tomanek, D., "Unusually High Thermal Conductivity of Carbon Nanotubes," Phys. Rev. Lett., vol. 84 (2000), pp. 4613-4616.

[6] Maruyama, S., Kojima, R., Miyauchi, Y., Chiashi, S., Kohno, M., "Low-Temperature Synthesis of High-Purity Single-Walled Carbon Nanotubes from Alcohol," Chem. Phys. Lett., vol. 360 (2002), pp. 229-234.

[7] Murakami, Y., Miyauchi, Y., Chiashi, S., Maruyama, S., "Characterization of Single-Walled Carbon Nanotubes Catalytically Synthesized from Alcohol," Chem. Phys. Lett., vol. 374 (2003), pp. 53-58.

[8] Murakami, Y., Yamakita, S., Okubo, T., Maruyama, S., "Single-Walled Carbon Nanotubes Catalytically Grown from Mesoporous Silica Thin Film," Chem. Phys. Lett., vol. 375 (2003), pp. 393-398.

[9] Murakami, Y., Miyauchi, Y., Chiashi, S., Maruyama, S., "Direct Synthesis of High-Quality Single-Walled Carbon Nanotubes on Silicon and Quartz Substrates," Chem. Phys. Lett., vol. 377 (2003), pp. 49-54.

[10] Maruyama, S., Murakami, Y., Shibuta, Y., Miyauchi, Y., Chiashi, S., "Generation of Single-Walled Carbon Nanotubes from Alcohol and Generation Mechanism by Molecular Dynamics Simulations," J. Nanoscience Nanotechnology, (2003), in press.

[11] Maruyama, S., Miyauchi, Y., Murakami, Y., Chiashi, S., "Optical Characterization of Single-Walled Carbon Nanotubes Synthesized by Catalytic Decomposition of Alcohol," New Journal of Physics, (2003), submitted.

[12] Maruyama, S., Miyauchi, Y., Edamura, T., Igarashi, Y., Chiashi, S., Murakami, Y., "Synthesis of Single-Walled Carbon Nanotubes with Narrow Diameter-Distribution from Fullerene," Chem. Phys. Lett., vol. 375 (2003), pp. 553-559.

[13] Maruyama, S., Choi, S.-H., "Molecular Dynamics of Heat Conduction through Carbon Nanotube," Therm. Sci. Eng., vol. 9 (2001), pp. 17-24.

[14] Maruyama, S., "A Molecular Dynamics Simulation of Heat Conduction in Finite Length SWNTs," Physica B, vol. 323 (2002), pp. 272-274.

[15] Maruyama, S., "A Molecular Dynamics Simulation of Heat Conduction of a Finite Length Single-Walled Carbon Nanotube, Micro. Thermophys. Eng., vol. 7 (2003), pp. 41-50.

[16] Yamaguchi, Y., Maruyama, S., "A Molecular Dynamics Simulation of the Fullerene Formation Process," Chem. Phys. Lett., vol. 286 (1998), pp. 336-342.

[17] Brenner, D.W., "Empirical Potential for

Hydrocarbons for Use in Simulating the Chemical Vapor Deposition of Diamond Films," Phys. Rev. B, vol. 42 (1990), pp. 9458-9471.

[18] Thess, A., Lee, R., Nikolaev, P., Dai, H., Petit, P., Robert, J., Xu, C., Lee, Y.H., Kim S.G., Rinzler, A.G., Colbert, D.T., Scuseria, G.E., Tomanek, D., Fischer, J.E., Smalley, R.E., "Crystalline Ropes of Metallic Carbon Nanotubes," Science, vol. 273 (1996), pp. 483-487.

[19] Journet, C., Maser, W.K., Bernier, P., Loiseau, A., Chapelle, M.L., Lefrant, S., Deniard, P., Lee, R., Fischer, J.E., "Large-Scale Production of Single-Walled Carbon Nanotubes by the Electric-Arc Technique," Nature, vol. 388 (1997), pp. 756-758.

[20] Dai, H., Rinzler, A.G.., Nikolaev, P., Thess, A., Colbert, D.T., Smalley, R.E., "Single-Walled Nanotubes Produced by Metal-Catalyzed Disproportionation of Carbon Monoxide," Chem. Phys. Lett, vol. 260 (1996), pp. 471-475.

[21] Nikolaev, P., Bronikowski, M.J., Bradley, R.K., Rohmund, F., Colbert, D.T., Smith, K.A., Smalley, R.E., "Gas-Phase Catalytic Growth of Single-Walled Carbon Nanotubes from Carbon Monoxide," Chem. Phys. Lett., vol. 313, (1999), pp.91-97.

[22]Bronikowski, M.J., Willis, P.A., Colbert, D.T., Smith, K.A, Smalley, R.E., "Gas-phase Production of Carbon Single-Walled Nanotubes from Carbon Monoxide via the HiPco Process: A Parametric Study," J. Vac. Sci. Technol. A, vol. 19 (2001), pp. 1800-1805.

[23] Colomer, J.F., Benoit, J.M., Stephan, C., Lefrant, S., Van Tendeloo, G., Nagy, J.B., "Characterization of Single-Wall Carbon Nanotubes Produced by CCVD Method," Chem. Phys. Lett., vol. 345 (2001), pp. 42-45.

[24] Alvarez, W.E., Kitiyanan, B., Borgna, A., Resasco, D.E., "Synergism of Co and Mo in the Catalytic Production of Single-Wall Carbon Nanotubes by Decomposition of CO," Carbon, vol. 39 (2001), pp. 547-558.

[25] Mukhopadhyay, K., Koshio, A., Tanaka, N., Shinohara, H., "A Simple and Novel Way to Synthesize Aligned Nanotube Bundles at Low Temperature," Jpn. J. Appl. Phys., vol. 37 (1998), pp. L1257-L1259.

[26]Mukhopadhyay, K., Koshio, A., Sugai, T., Tanaka, N., Shinohara, H., Konya, Z., Nagy, J. B., "Bulk Production of Quasi-Aligned Carbon Nanotube Bundles by the Catalytic Chemical Deposition (CCVD) Method," Chem. Phys. Lett., vol. 303 (1999), pp. 117-124.

[27] Rao, A.M., Richter, E., Bandow, S., Chase, B., Eklund, P.C., Williams, K.A., Fang, S., Subbaswamy, K.R., Menon, M., Thess, A., Smalley, R.E., Dresselhaus, G., Dresselhaus, M.S., "Diameter-Selective Raman Scattering from Vibrational Modes in Carbon Nanotubes," Science, vol. 275 (1997), pp. 187-191.

[28] Dresselhaus, M.S., Eklund, P.C., "Phonons in Carbon Nanotubes," Adv. Phys., vol. 49 (2000), pp. 705-814.

[29] Jorio, A., Saito, R., Hafner, J.H., Lieber, C.M., Hunter, M., McClure, T., Dresselhaus, G., Dresselhaus, M.S., "Structural (n, m) Determination of Isolated Single-Walled Carbon Nanotubes by Resonant Raman Scattering," Phys. Rev. Lett., vol. 86 (2001), pp. 1118-1121.

[30] Saito, R., Dresselhaus, G., Dresselhaus, M.S., "Trigonal Warping Effect of Carbon Nanotubes," Phys. Rev. B, vol. 61 (2000), pp. 2981-2990.

[31] Maruyama, S., "Molecular Dynamics Method for Microscale Heat Transfer," Advances in Numerical Heat Transfer, vol. 2 (2000), pp. 189-226.